BAU Journal - Science and Technology

Volume 4 | Issue 2
ISSN: 2959-331X

Article 10

June 2023

THE INFLUENCE OF BIO-INHIBITOR ON THE CORROSION RESISTANCE OF REINFORCED CONCRETE BEAMS CONTAINING MSWI-BA AS A PARTIAL SAND REPLACEMENT

Jamal Khatib
Faculty of Engineering, Beirut Arab University, Debbieh, Lebanon, j.khatib@bau.edu.lb

Israa Amer
Faculty of Engineering, Beirut Arab University, Debbieh, Lebanon, isa061@student.bau.edu.lb

Ghanem Hassan
Faculty of Engineering, Beirut Arab University, Debbieh, Lebanon, h.ghanem@bau.edu.lb

Adel Elkordi
Faculty of Engineering, Beirut Arab University, Debbieh, Lebanon, a.elkordi@bau.edu.lb

Recommended Citation

Khatib, Jamal; Amer, Israa; Hassan, Ghanem; and Elkordi, Adel (2023) "THE INFLUENCE OF BIO-INHIBITOR ON THE CORROSION RESISTANCE OF REINFORCED CONCRETE BEAMS CONTAINING MSWI-BA AS A PARTIAL SAND REPLACEMENT," *BAU Journal - Science and Technology*: Vol. 4: Iss. 2, Article 10.
DOI: https://doi.org/10.54729/2959-331X.1102

1. INTRODUCTION

Today, reinforced concrete is a common construction material used around the globe. Among the primary causes of RC constructions, degrading over time is the corrosion of the reinforcement bars **(Angst et al., 2018)**. Despite steel has a natural inclination to corrode, concrete has an alkaline pore solution PH of 13–14 **(Fu, C. et al., 2017)**, which naturally passivizes embedded reinforcement steel. On the surface of embedded steel, a protective passive layer forms. This layer, that is self-generated, appears shortly after cement hydration begins. The rebar stays undamaged as long as that oxide layer is maintained. Carbon dioxide gas can permeate the concrete and interact with different cement hydration products, lowering the PH of alkaline solution present in the pores of hardened concrete dramatically **(Turcry et al., 2014)**.

Most buildings are chloride-contaminated because of deicing throughout the winter, as well as in chloride-laden conditions such as the sea for marine buildings **(Nguyen et al., 1991)**. The fundamental activity of chlorides is to generate corrosion of reinforcing steel and cause the damage of surrounding concrete. Chloride ions degrade the coating and corrosion take place in the existence of water and oxygen (**Malumbela et al., 2012).** The curing duration and the water to cement ratio are the two key factors that affect the concrete penetrability **(Ghanem, H. et al., 2008).** As the curing duration increases, the chloride penetrability decreases **(Ghanem, H. et al., 2018).**

Corrosion process reduces the cross-sectional area of reinforcement bars and increases their mass, resulting in decreased in its mechanical characteristics and a deterioration of the bond properties between steel and concrete **(Abou Shakra et al., 2020)**. Consequently, corrosion of reinforcement bars becomes a significant factor of RC buildings durability, resulting in financial loss and repair costs **(Zhu et al., 2016). Adukpo, E. et al., (2013)** studied the influence of mild steel bar corrosion on the tensile strength, bond strength, and bending strength of a RC beam. The results showed that the corrosion of steel rebar minimized its tensile strength, affected its bonding with concrete and minimized the flexural capacity of steel-reinforced concrete. Another study was conducted by **S. Imperatore et al., (2008)** to examine the corrosion impacts on steel reinforcing bars and at the steel-concrete interface, concluded that the corrosion affected the reinforcement shape and decreased its diameter.

Corrosion inhibitors are chemical substances that, while exist in sufficient quantities, can eliminate or minimize corrosion rate. The usage of inhibitors appears to be more viable due to their ease of application and low cost (**Elsener et al., 2001)**. Furthermore, several admixtures that have been shown to be efficient at reducing corrosion of steel, like nitrite but it is being banned in many nations due to its toxicity and environmental problem **(Shi et al., 2014)**. The investigation for ecologically benign substitutes that are efficient rather than the well-known harmful corrosion inhibitors is a new trend in corrosion prevention research **(Afia et al., 2013)**. The green corrosion inhibitors such as plant extracts are commonly found in many countries. These inhibitors are inexpensive, simple to manufacture, harmless, biodegradable, and eco-friendly. They can produce protective coatings on the surface of the metal of the steel bars by coordinating with metal cations, preventing the corrosion mechanism from progressing **(Shahid et al., 2011). Quraishi et al., (2011)** developed a green corrosion inhibitor called Calcium stearate and studied its inhibition effect on steel corrosion. The study showed that calcium stearate's excellent effectiveness demonstrated its potential for corrosion reduction. **Harb et al., (2020)** conducted a study to determine the inhibition activity of Olea europaea L. extracts on corrosion of mild steel. It was found that the use of these leaves provided efficient protection against corrosion for steel in RC designed for sea environments.

Municipal solid waste (MSW) has been increased globally by rapid population growth. Two billion tons of MSW were produced globally in 2016. It is anticipated that this amount will rise significantly in the coming years **(dos Santos et al., 2020)**. Governments and countries are paying close attention to this troublesome problem because of the massive output of MSW, which has the potential to seriously harm both the environment and public health. As a result, the need for an efficient method of recycling these wastes becomes global. Recycling, disposal of solid waste, or incineration **(Tang Z et al., 2020, Liu J et al., 2021)** are the standard methods for treating MSW. Incineration is among the most efficient MSW disposal technologies, with the benefits of decreasing and reusing waste material **(Garcia-Lodeiro et al., 2016)**. As a result, two major solid

by-products: fly ash and bottom ash are created following the burning process. MSWI-BA is the major by-product, representing 25-30% by mass and 10% by volume of burned waste **(Lam et al., 2010).** It includes far fewer leachable contaminants and extremely hazardous organic compounds, like dioxins, than incinerated fly ash **(Ferreira et al., 2003)**. In addition, bottom ash has a negligible chloride level and so has the ability to be employed in the production of concrete mixes **(Pavlík et al., 2011).** MSWI-BA has the ability to be used as aggregate or cement in concrete mixture, providing an excellent application of the ash **(Baalbaki et al., 2019, Machaka et al., 2019). Khatib, j. et al., (2021)** studied the structural properties of RC beams containing MSWI-BA. The obtained results bending tests revealed that the beam containing BA20 had the best load capacity and ductility. Meanwhile, as the amount of BA above 20%, the load capacity and ductility of the material dropped. **Ghanem et al., (2019)** evaluated the possible use of MSWI-BA as a partial cement substitute in mortar specimens. It was found that the use of MSWI-BA reduced the compressive strength and limited the pozzolanic activity.

The present research investigates the effect of using MSWI-BA as a partial sand replacement and Ceratonia siliqua extract as a green corrosion inhibitor on the structural behavior of reinforced concrete beams in normal conditions and in the presence of corrosion. Four mixes were prepared with/without MSWI-BA and with/without Ceratonia siliqua extract to prepare eight beams. The density, UPV, compressive strength, split tensile strength and elastic modulus were determined. In addition, the load deflection and strain of RC beams were determined. Four beams were exposed to accelerated corrosion test and four beams were kept at the ambient temperature.

2. METHODOLOGY

2.1 Material

The cement used was ordinary Portland cement complied with Lebanese standards (NL53). The coarse aggregate (CA) was limestone with a nominal particle size 9.5 mm. The specific gravity was 2.55. The water absorption was 2.49 %. Natural sand was used as a fine aggregate (FA) with a maximum particle size 4.75 mm. The specific gravity was 2.57. The water absorption was 2.48 %.

The MSWI-BA was received in a powder form from MSWI plant located in Beqaa area. The maximum particle size was 4.75 mm. The specific gravity was 1.5 and the water absorption was 17 %. MSWI-BA was soaked in water for 7 days with liquid to solid ratio equal to 5. This step is necessary to remove any contaminants like heavy metals and chloride. Each day, MSWI-BA were strung for 10 minutes and were leaved to settle to the next day. Then all particles were dried in the oven at 100°c. The particle size distribution of MSWI-BA, sand and coarse aggregates are shown in fig.1.

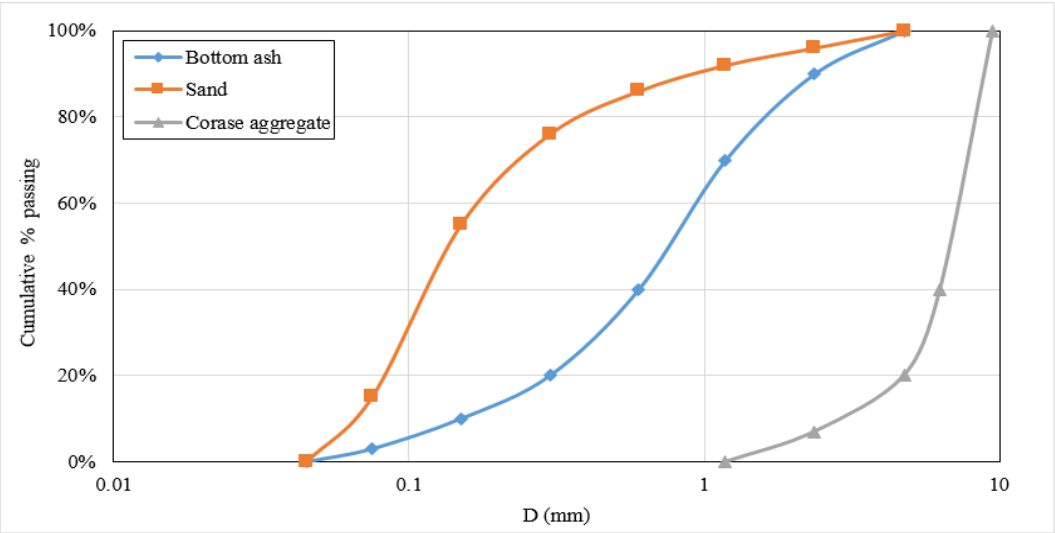

Fig.1: Particle size distribution of MSWI-BA, sand and coarse.

2.2 Mix Design

Four concrete mixes were prepared. The proportion of control mix was 1:2:4 (cement: FA: CA). The percentage of inhibitor used was 1.5% by weight of cement. Fine aggregates were replaced with 20% MSWI-BA. R0 referred to control mix, R0+I to control mix + Ceratonia siliqua extract, R20 to 20% replacement of sand and R20+I to 20% replacement of sand + Ceratonia siliqua extract. The water to cement ratio was 0.5. The mixing water content for mixes containing MSWI-BA increases due to the high water absorption of MSWI-BA. All details are presented in table 1.

Table 1: Details of concrete mixes (Kg / m^3)

sample	% of replacement	Cement	FA	CA	Water	MSWI-BA	Bio inhibitor
R0	0	317	634	1268	159	0	0
R0+I	0	317	634	1268	159	0	4.76
R20	20	317	507	1268	143	127	0
R20+I	20	317	507	1268	143	127	4.76

2.3 Reinforced Concrete Beam Design

RC beams of dimensions 100x200x1000 mm were prepared (fig.2). Two mild steel bars had a diameter 6 mm were used for top reinforcement and another two mild steel bars of 8 mm diameter for bottom reinforcement with stirrups of 6 mm diameter spaced at 10 cm. For accelerated corrosion test, three steel bars were linked to steel cage to let the current flow throw all bars with the same value.

(a) (b)

Fig.2: Beam reinforcement details; (a) for beams in normal condition and (b) for beams exposed to accelerated corrosion.

2.4 Sample Preparation

All material quantities were calculated for all mixes and then weighed based on their proportions. During mixing, CA is firstly placed then FA and cement. These materials were mixed before adding water and continued mixing until obtaining a homogenous mix. The slump test was conducted to check the workability. The slump value was 15.5 cm, 17 cm, 15 cm and 16.5 cm for R0, R0+I, R20 and R20+I respectively. Cubes of 10x10x10 cm were cast to measure the UPV and compressive strength. Cylinders of 15x30 cm were cast to measure the elastic modulus and the split tensile strength. Beams were cast to examine the flexural behavior of concrete (fig.3). For each mix, nine cubes, two cylinders and two beams were cast. All specimens were cured in water until testing.

Fig.3: Casted beams and cubes

2.5 Inhibitor Preparation

2.5.1 Preparation of plant material

Ceratonia siliqua l. **(Ceratonia siliqua)** leaves were collected from **Debbieh in Ikleem Al Kharroub, Lebanon.** The sample was washed, oven-dried at 60° C for 4-6 hours until complete dehydration, and then ground into powder using a blender (fig.4). The powdered sample was stored in an air-tight bag at 20° C.

(a) (b) (c)

Fig.4: Preparation of plant material. (a): Washing Ceratonia siliqua leaves, (b): Drying Ceratonia siliqua leaves, (c): Grinding Ceratonia siliqua leaves.

2.5.2 Preparation of plant extract

The powdered sample of plant material (240 g of sample) was extracted in 1200 mL of distilled water under reflux at 95° C for 6 hours for 3 times (fig.5). Vacuum filtration was carried out using Buchner funnel via Whatman filter paper No 2. The crude extracts were stored at 4°C in air-tight brown bottles for future use.

Fig.5: Experimental setup of extracting

2.6 Accelerated Corrosion Test

The accelerated corrosion test was performed on four beams R0 C, R0+I C, R20 C and R20+I C. The letter "C" refers to beams exposed to accelerated corrosion test. As shown in fig.6, all beams were placed in a curing tank containing 5% NaCl solution for 28 days until they attain the designed concrete compressive strength. A stainless steel was immersed with the reinforced beams. At the start of the test, every beam was connected to a DC power supply producing a current of 1.5A for 3 weeks. The reinforcement bars represent the anode and the stainless steel plate represents the cathode. When the current was turned on, the steel bars within the beams began to corrode. It was noted that the tank solution color changes to a darker rusty. This is probably caused by the steel bar ions leaching out as a result of the electrochemical reactions occurring.

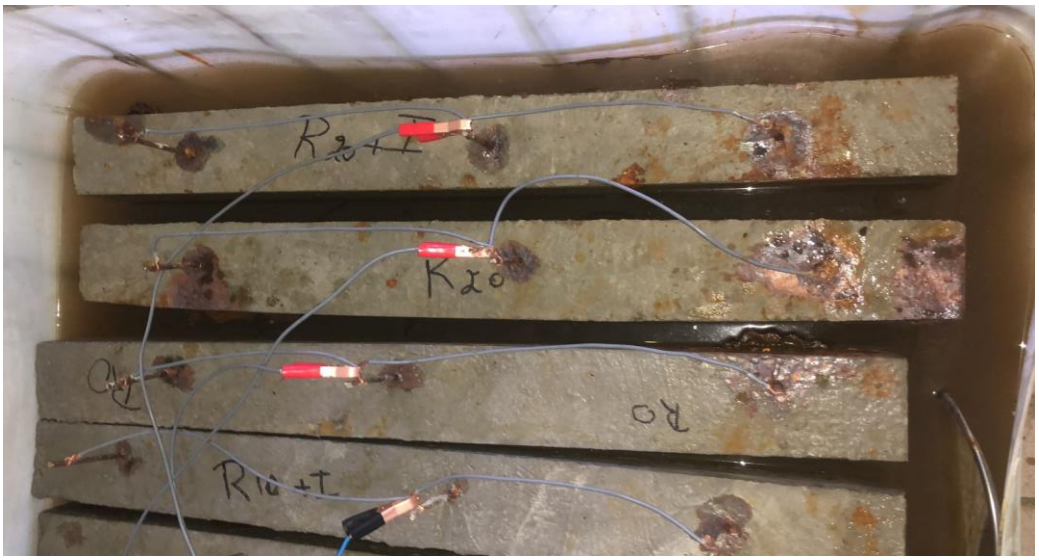

Fig.6: Experimental setup of accelerated corrosion of reinforced concrete beams.

2.7 Testing

The density, UPV and the compressive strength test were conducted at 1, 7 and 28 days of curing according to ASTM C138, ASTM C597 and ASTM C39 respectively. Concrete's elastic modulus and split tensile strength was measured according to ASTM C469 and ASTM C496 respectively. A three-point bending flexural test was conducted to study the flexural behavior of reinforced concrete beams according to ASTM C78. As shown in fig.7, a 5 kN load was applied at the mid span of the beam until yielding occurred. The machine was halted at every load to record the center deflection and the strain at various loads. The initial crack load was noted. Throughout testing, cracks were seen to spread.

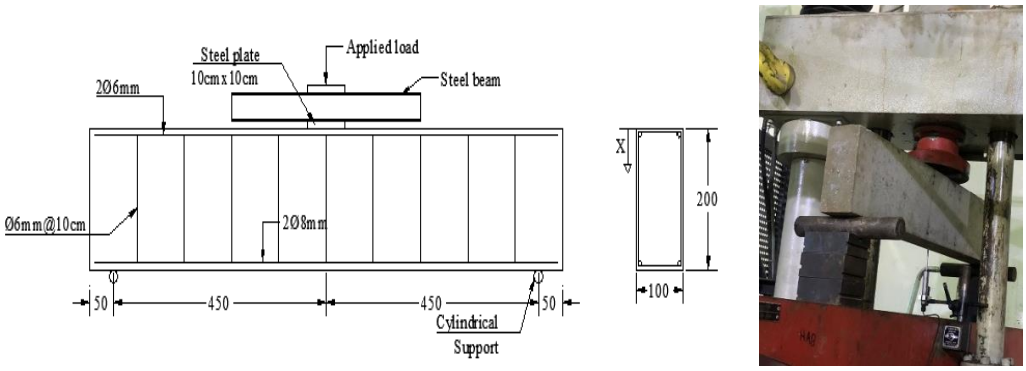

(a) (b)

Fig.7: Three point bending test: (a) beam dimensions and reinforcement, (b) test machine.

3. RESULTS

3.1 Concrete Properties

3.1.1 Density

Density results are shown in fig.8. Each value was the average of three replicate samples. As shown in the figure, the densities of concrete after 28 days of curing were 2510 Kg/m^3, 2540 Kg/m^3, 2330 Kg/m^3 and 2359 Kg/m^3 for R0, R0+I, R20 and R20+I respectively. When 20 % of sand was replaced by MSWI-BA, the density decreased about 7%. This is due to the fact that MSWI-BA has a lower density than the fine aggregate. Another point can be deduced that the use of Ceratonia siliqua extract doesn't affect the density. For example, the density of R0+I was 2540 Kg/m^3 and for R0 it was 2510 Kg/m^3.

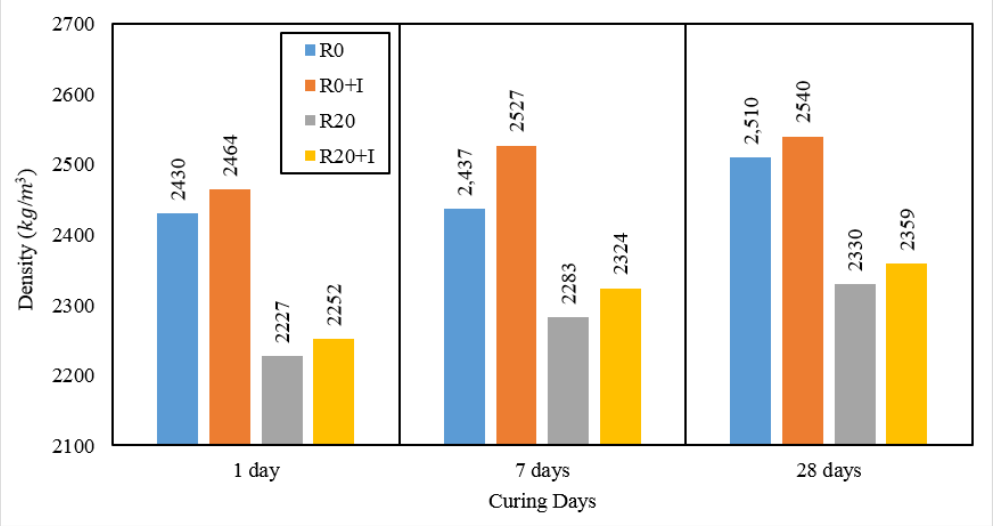

Fig.8: Density of cube specimens

3.1.2 Ultrasonic Pulse Velocity

Ultrasonic pulse velocity test is a non-destructive test to evaluate the uniformity of concrete and the presence of voids. The classification of the quality of concrete is shown in table 2. UPV test was conducted at day 1, 7 and 28.

Table 2: Classification of the quality of concrete based on UPV (Machaka et al., 2019)

Pulse Velocity	Quality of Concrete
>4.5 km/s	Excellent
3.5 – 4.5 km/s	Good
3.0 – 3.5 km/s	Doubtful
2.0 – 3.0 km/s	Poor
<2.0	Very poor

UPV results are presented in fig.9. Each value was the average of three replicate samples. As shown, the values of all mixes show a good quality of concrete. It means that the inclusion of MSWI-BA and Ceratonia siliqua did not affect negatively the concrete quality. The use of MSWI-BA lead to a reduction in UPV values due to the light specific gravity and the increase in voids ratio. The reduction was 7.3%. However, the use of Ceratonia siliqua extract doesn't appear that has a negative effect in UPV results. For example, at 28 days the reduction in UPV value was 1.3%.

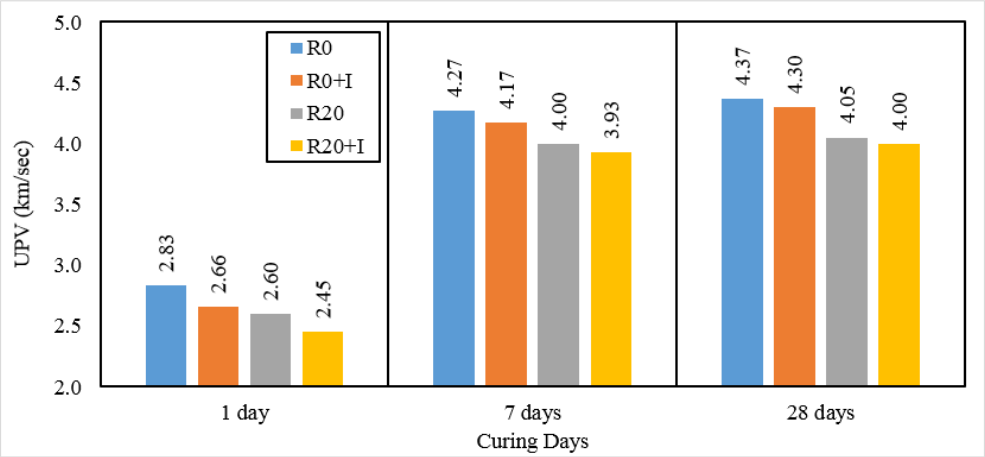

Fig.9: UPV for cubic specimens

3.1.3 Compressive Strength

The compressive strength results are displayed in fig.10. The results showed the average of three replicate samples. As shown, the control mix have the highest compressive strength at all ages. At 28 days, the compressive strengths were 26.7 MPa, 23.1 MPa, 21 MPa and 19 MPa for R0, R0+I, R20 and R20+I respectively. The results show that replacing 20% of sand by MSWI-BA decreases the compressive strength about 16%. This may be because of the heavy metals and toxic minerals existing in the MSWI-BA. Another point can be deducted that the use of Ceratonia siliqua extract also reduces the compressive strength. The reduction was about 14%. The same behavior is shown at 1 and 7 days. The concrete strengths at 7 days were 17.8 MPa, 14.8 MPa, 13.5 MPa and 11.5 MPa for R0, R0+I, R20 and R20+I respectively.

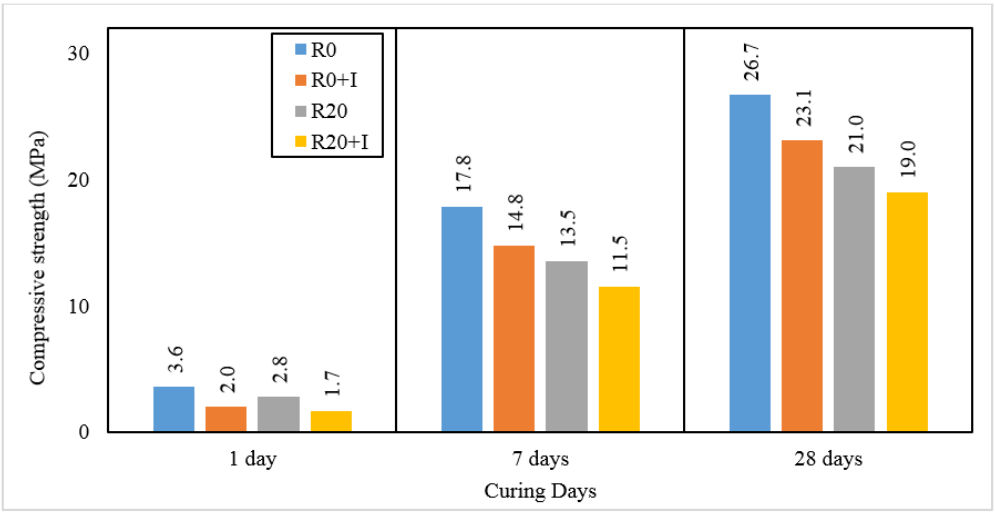

Fig.10: Compressive strength for cubic specimens

3.1.4 Elastic Modulus (E)

Results of elastic modulus are presented in fig.11. The results represented the average of two replicate samples. As for E, the control mix R0 showed the highest E (24411 MPa). It can be noticed that replacing the fine aggregate by MSWI-BA decreases E. For example, E of R0+I was 22563 MPa whereas for R20+I it was 20487 MPa. In addition, adding Ceratonia siliqua extract to concrete mix leads to a slight reduction. For example, E of R20 was 21538 MPa whereas it was 20487 MPa for R20+I.

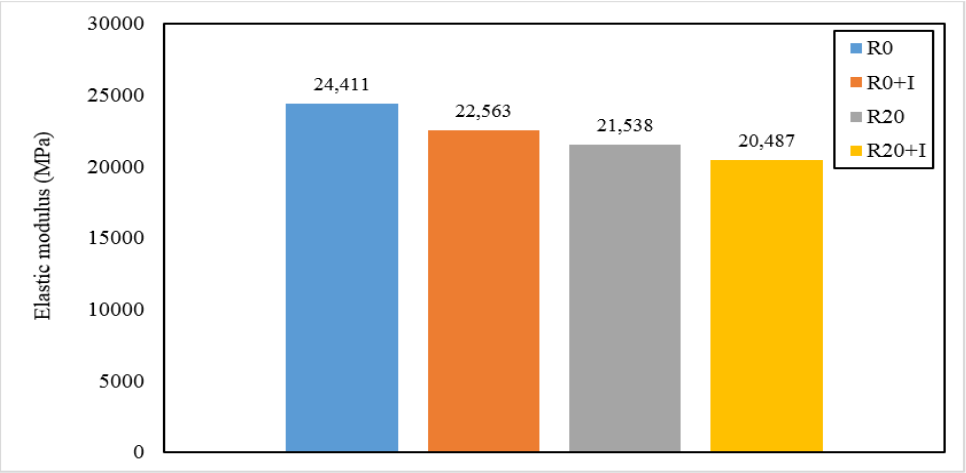

Fig.11: Elastic modulus for cylindrical specimens

3.1.5 Tensile Strength

Results of tensile strength are shown in fig.12. The average of the two replicate samples tested is depicted in fig.12. Similar trend for split tensile strength, when 20% of fine aggregate was replaced by MSWI-BA the tensile strength decreased. For example, the strength of R0 was 2.55 MPa whereas for R20 it was 2.39 MPa. Furthermore, adding Ceratonia siliqua extract to concrete mix reduces the tensile strength. For example, for mix containing MSWI-BA the reduction was 13.6%.

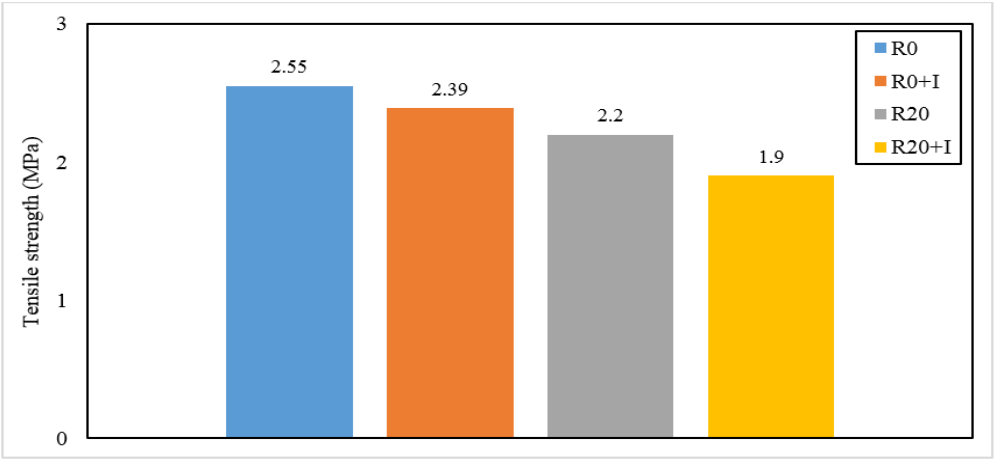

Fig.12: Tensile strength for cylindrical specimens at 28 days

3.2 Effect of MSWI-BA and Corrosion Inhibitor on the Behavior of RC Beams

3.2.1 Load deflection

The load deflection curves of all beams are plotted in fig.13 and fig.14. As shown, the highest performance in terms of load carrying capacity was demonstrated by beam R0. R0 reaches a maximum capacity at 33 kN. Subsequently, cracks propagated due to the reduction of beam stiffness. Prior to failure when the large deflection was observed, the test was stopped. On the other side, R0+I was slightly lower than R0 (around 9%) as shown in fig.13. This is obvious due to the presence of Ceratonia siliqua extract.

In comparison to R0, the load capacity of the two other beams, which were exposed to accelerated corrosion (R0 C and R0+I C) decreased. The reduction was around 30% and 21.7% for R0 C and R0+I C respectively which means that the corrosion reduces the ultimate load capacity of beams verifying what earlier research has demonstrated **(Hakim, A et al 2022).**

But in case of using the Ceratonia siliqua extract as green inhibitor in the beam exposed to accelerated corrosion test (R0+I C), the reduction in load capacity was

lower than the beam that does not contain Ceratonia siliqua extract (R0 C), which mean that this inhibitor has a role in protecting steel from corrosion. However, in normal circumstances, the Ceratonia siliqua extract does not have any effect on protecting steel reinforcement and increasing the ultimate load capacity.

From fig.14, it should be noted that R20 has the highest load capacity 26.4 kN in comparing to R20+I, R20 C and R20+I C, which they reached 25 kN, 22.5 kN, and 23.48 kN respectively. The ultimate load capacity for beam containing MSWI-BA (R20) was lower than R0. It means that the use of MSWI-BA reduces the load carrying capacity due to the presence of contaminants. When adding Ceratonia siliqua extract, the load capacity decreased to 25 kN. As well for beams exposed to corrosion, the reduction was around 14.77% and 11% for R20 C and R20+I C respectively. However, the ultimate load capacity for R20+I C was higher than R20 C making a slight increase by 4.25%.

The load deflection curve consisted of three zones:

1- An elastic zone characterizing the rising area where the load applied and the deflection are linearly proportionate up to the initial micro crack. As the load increases, the deflection increases.
2- The plastic zone begins beyond the initial crack point. It includes the remaining rising part, where the load applied rises as the displacement rises. At the end of this stage, the beam has reached its maximum capacity, when cracks developed.
3- The post-cracking zone when the beam hits its maximum capacity, the damaged area begins to indicate the beam's stiffness loss. In this zone, the stiffness decreases as the applied load increases until the rapture of reinforcement bars.

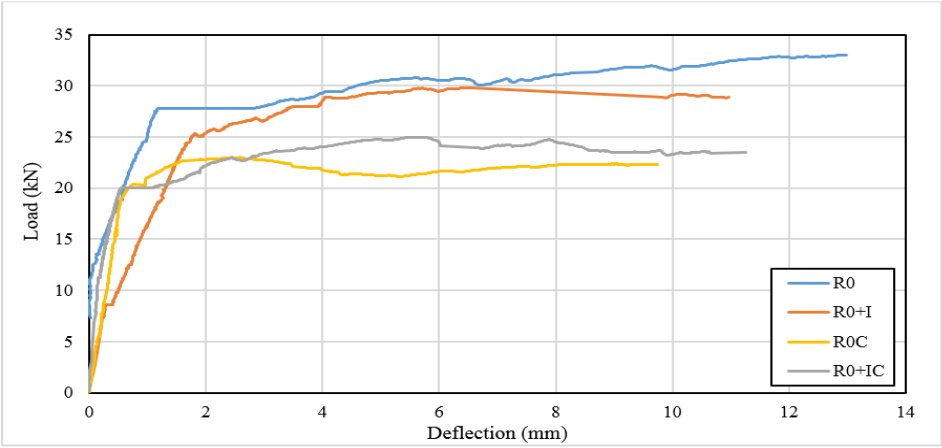

Fig.13: Load deflection curves for control beams

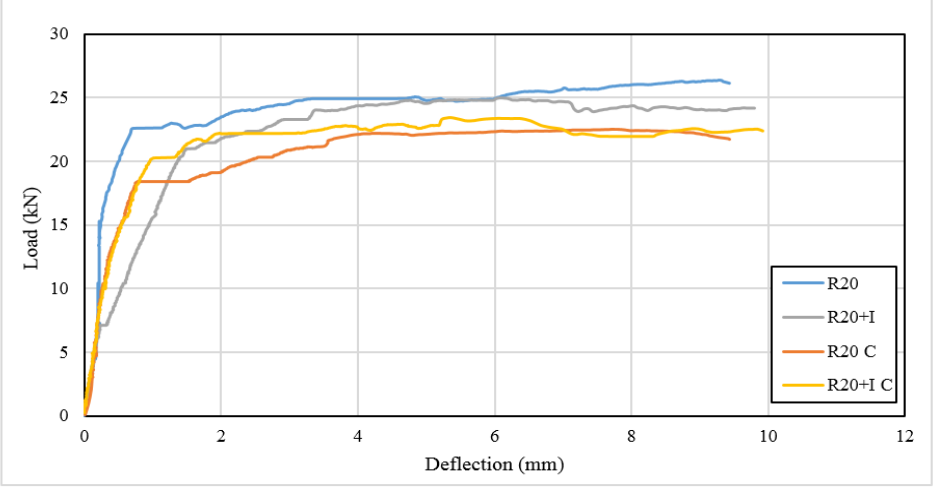

Fig.14: Load deflection curves for beams containing MSWI-BA

3.2.2 Failure behavior

All beams exhibit a common pattern of failure as the load on the testing machine rises. As shown in fig.15 and fig.16, flexural cracks begin almost at the bottom of the center of beam. It should be highlighted that the corroded beams have wider and more flexural cracks. These cracks start in the mid-span of the beam and grow quicker in width as they move from the bottom (tension area) to the top (compression area).

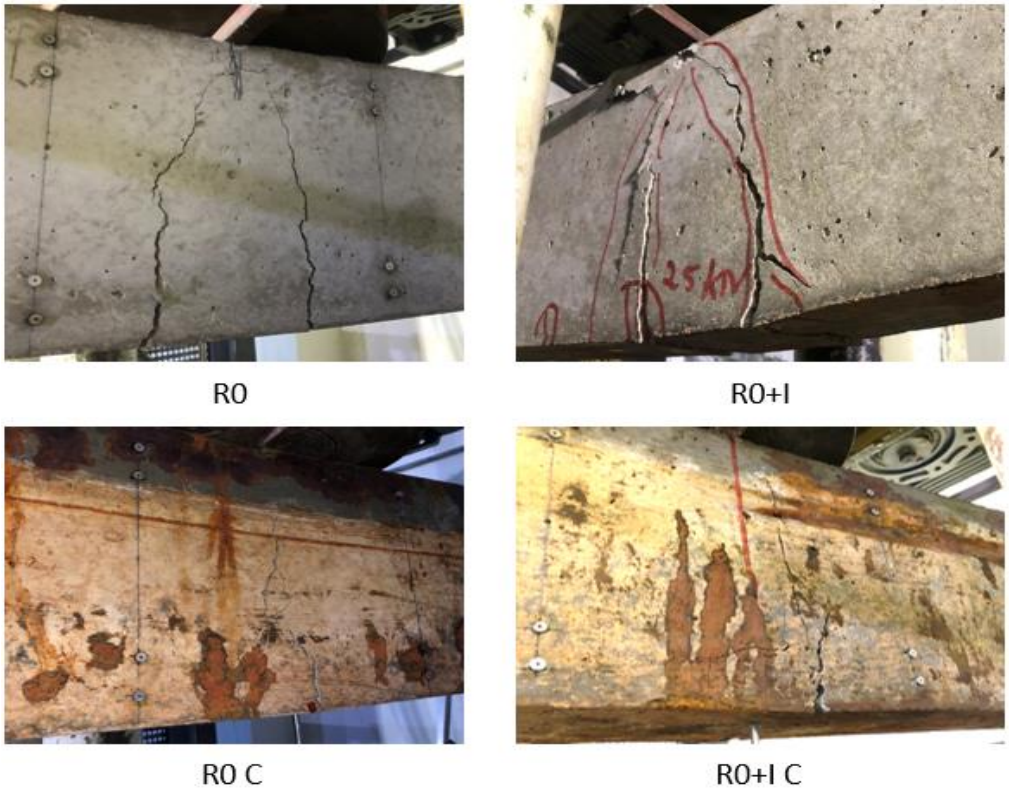

Fig.15: Cracks pattern for control beams

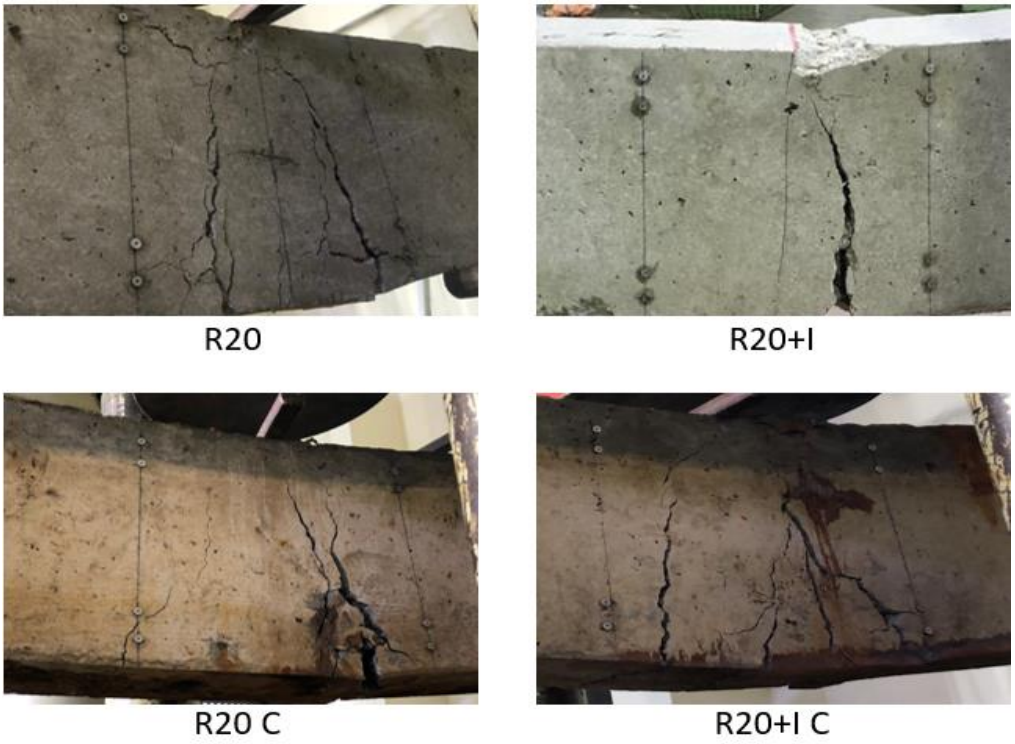

Fig.16: Cracks pattern for beams containing MSWI-BA

As shown in fig.17, the first crack appears earlier for beams that have low strength. For example, the strength of R20 was lower than R0, therefore the first crack of R20 appeared at 23 kN whereas for R0 at 27 kN. Furthermore, cracks appeared at a lower load for all beams that were subjected to corrosion in comparing to other beams. For example, the first crack appears at 23 kN for R20 and at 18 kN for R20 C.

In addition, Ceratonia siliqua extract has no effect on cracks appearance for uncorroded beams. However, for corroded beams, the first crack appears earlier in beams without Ceratonia siliqua extract. This indicates that the inhibitor has an effect on increasing the load capacity of corroded beams. For example, for R0 C the first crack appeared at 19.2 kN, but for R0+I C it appeared at 22 kN.

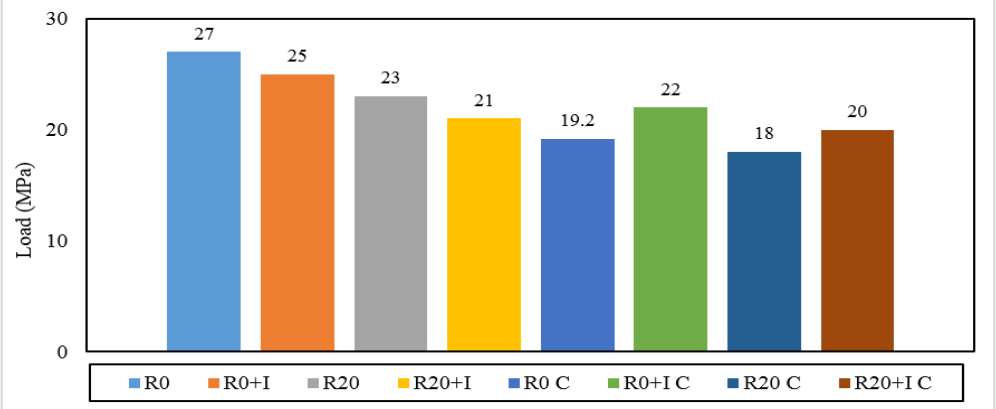

Fig.17: Load at first crack for all beams

3.2.3 Strain measurements

Four pairs of demic points were placed along with the depth of the beam to study the strain distribution at different points (20, 40, 160 and 180 mm). The strain distribution at various load increments (5, 10 and 15 kN) are shown in fig.18 and fig.19. In all cases, when the load on beam increases the strain increases.

Regarding control beams, R0 have a lower strain than R0+I. For example, when applying load of 15 kN the strain at the bottom of the beam was 0.0004 mm for R0 and 0.00057 mm for R0+I. This is consistent with beam R0+I having higher central displacements than the control beam under the same load. This might be because beam R0+I have less elastic modulus than R0.

For beams containing MSWI-BA, R20 and R20+I, the strain value for R20+I is larger than R20, also because R20 have a higher elastic modulus than R20+I. In comparing control beams and beams containing MSWI-BA, all beams with MSWI-BA show larger strain, this indicate that the use of MSWI-BA lead to increase the strain also because they have lower elastic modulus than the beams without MSWI-BA. For example, the strain at the bottom of the beam of R20 when applying 10 kN was 0.00024 mm higher than R0 which attain 0.00015 mm.

In comparing beams in normal conditions and beams under accelerated corrosion test, it shows that corrosion leads to an increase in strain. For example, when applying 15 kN, the strain of R0 at a depth 160 mm was 0.00034 mm whereas for R0 C it was 0.0008 mm. However, when using the Ceratonia siliqua extract in beams exposed to accelerated corrosion test R0+I C and R20+I C the strain was lower than the beam without Ceratonia siliqua extract R0 C and R20 C. This means that the inhibitor protected steel from corrosion and reduced the strain. At 5 kN, the strain at 180 mm of R20+I C was 0.001 mm and 0.0012 mm for R20 C.

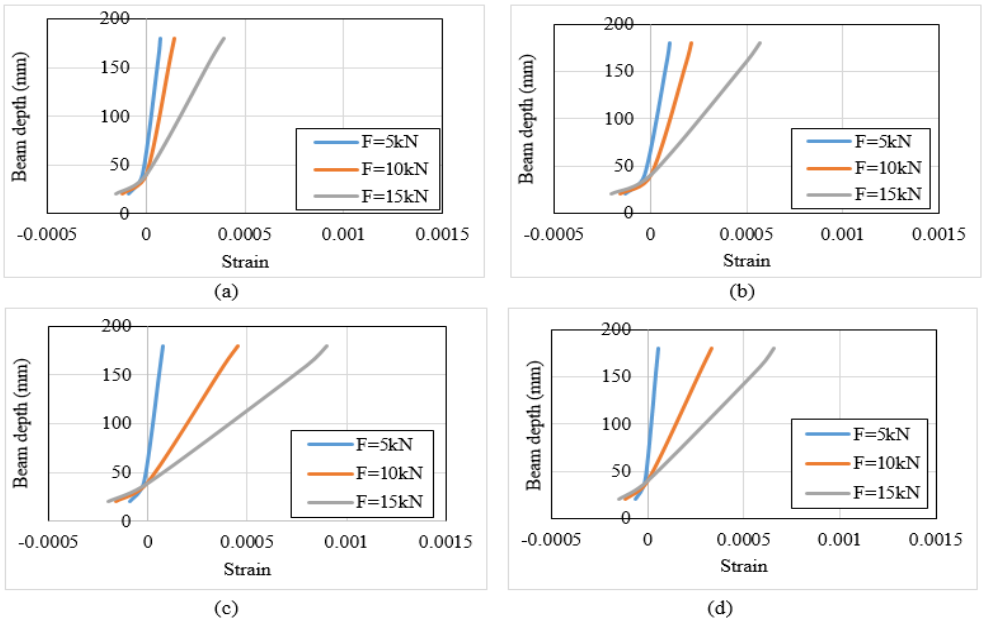

Fig.18: Strain measurement for control beams. (a): R0, (b): R0+I, (c): R0 C, (d): R0+I C.

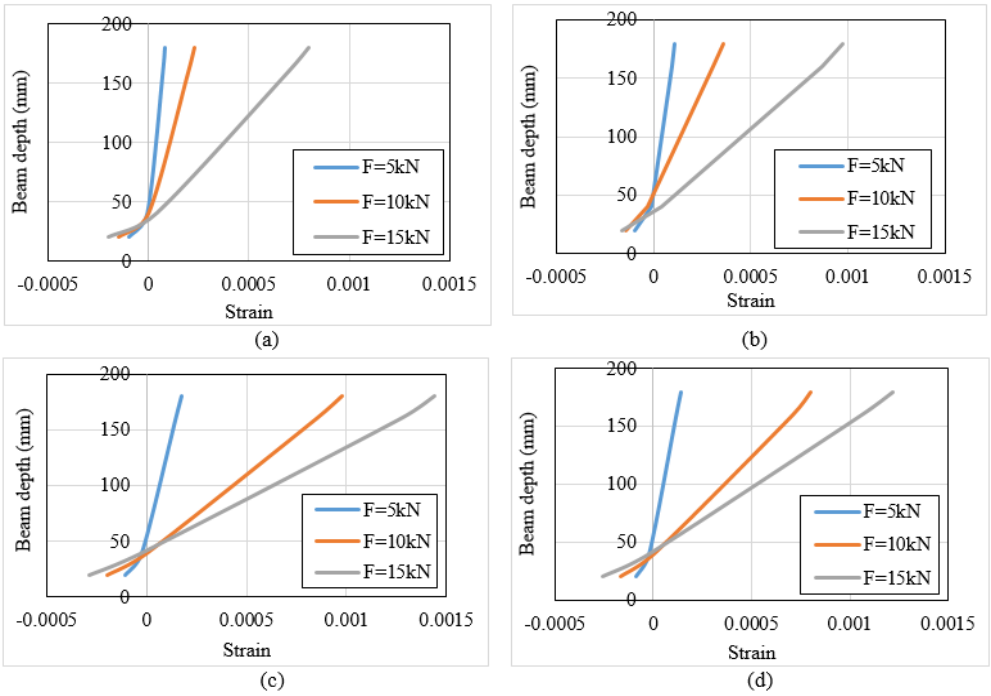

Fig.19: Strain measurement for beams containing MSWI-BA. (a): R20, (b): R20+I, (c): R20 C, (d): R20+I C.

3.2.4 Degree of corrosion

Following the flexural test, all corroded beams have their individual percentage of mass loss in reinforcing steel determined. This was accomplished by removing the tensile bars, mechanically brushing them. By measuring the residual mass, m, in comparison to the first measured mass, m_0, this enables an accurate estimate of the corrosion degree.

$$\%\ \text{Mass loss} = \left(\frac{m_0 - m}{m_0}\right) \times 100$$

The results illustrated in table 3 show that corrosion attacks the beams without inhibitor more than the beams containing Ceratonia siliqua extract, which mean that Ceratonia siliqua extract, has a role in protecting steel reinforcement from corrosion

and reducing mass loss. For example, the % mass loss of R0 C was 24.5% whereas for R0+I C it was 10.6%.

Table 3: Estimated mass loss in steel due to corrosion

Mixes	Nominal mass of steel cage (kg)	Residual mass of steel cage (g)	% Mass loss
R0 C	3.02	2.28	24.5%
R0+I C	3.02	2.7	10.6%
R20 C	3.02	2.42	19.86%
R20+I C	3.02	2.62	13.24%

4. CONCLUSIONS

The influence of using MSWI-BA as a partial sand replacement and Ceratonia siliqua extract as a green corrosion inhibitor on the structural behavior of RC beams was investigated. In this study, several conclusions can be made:

1- It was shown that replacing sand by MSWI-BA led to a slight decrease in workability and density of concrete. Furthermore, concrete with MSWI-BA showed a decrease in UPV, compressive strength, tensile strength and elastic modulus. However, the use of Ceratonia siliqua extract as corrosion inhibitor improved the workability of concrete. On the other hand, Ceratonia siliqua extract reduced the compressive strength, splitting tensile strength and elastic modulus.

2- Based on the three-points bending test, the replacement of sand by MSWI-BA (20%) decreased the load carrying capacity and the ductility of concrete beams. In terms of corrosion, all beams exposed to accelerate corrosion test showed a reduction in load carrying capacity.

3- In presence of corrosion, the load capacity of beams that contain Ceratonia siliqua extract as green corrosion inhibitor was higher than beams without Ceratonia siliqua extract. However, in absence of corrosion, the intrusion of Ceratonia siliqua extract led to reduce the load capacity.

4- The findings of structural damage revealed that all beams failed in flexure. For each beam, the crack intensity varied, though.

5- Strain measurements revealed that, for the same load value, the control beam showed lower strain values. Furthermore, the use of MSWI-BA increased the strain values. However, the strain values for beams exposed to corrosion were higher than beams that were not subjected to accelerated corrosion test. In addition, the use of Ceratonia siliqua extract in presence of corrosion reduced the strain values but in absence of corrosion, the strain values increased.

6- In terms of mass loss, the results showed that the Ceratonia siliqua extract reduces the percentage of mass loss.

7- Future research could include the use of different percentages of Ceratonia siliqua extract to select the best one in protecting steel reinforcement from corrosion.

REFERENCES

- Abou Shakra, J., Joumblat, R., Khatib, J., & Elkordi, A. (2020). Corrosion of coated and uncoated steel reinforcement in concrete. BAU Journal-Science and Technology, 2(1), 4.
- Adukpo, E., Oteng-Seifah, S., Manu, P., & Solomon-Ayeh, K. (2013). The effect of corrosion on the strength of steel reinforcement and reinforced concrete. Construction and Building Materials, 166-175.
- Afia, L., Salghi, R., Zarrouk, A., Zarrok, H., Bazzi, E. H., Hammouti, B., & Zougagh, M. (2013). Comparative study of corrosion inhibition on mild steel in HCl medium by three green compounds: Argania spinosa press cake, kernels and hulls extracts. Transactions of the Indian Institute of Metals, 66(1), 43-49.
- Angst, U. M. (2018). Challenges and opportunities in corrosion of steel in concrete. Materials and Structures, 51(1), 1-20.

- ASTM C39 / C39M Standard Test Method for Compressive Strength of Cylindrical Concrete Specimens.
- ASTM C469/C469M-14 Standard Test Method for Static Modulus of Elasticity and Poisson's Ratio of Concrete in Compression.
- ASTM C496/C496-17 American Society for Testing and Materials (2017), Standard Test Method for Splitting Tensile Strength of Cylindrical Concrete Specimens.
- ASTM C597, 2016 Edition, April 1, 2016 - Standard Test Method for Pulse Velocity through Concrete.
- ASTMC138/C138M, A. S. for T. and M (2017), 17a Standard test method for density (unit weight), yield, and air content (gravimetric) of concrete.
- ASTM-C78 Standard Test Method for Flexural Strength of Concrete (Using Simple Beam with Third-Point Loading
- Baalbaki, O., Elkordi, A., Ghanem, H., Machaka, M., & Khatib, J. M. (2019). Properties of concrete made of fine aggregates partially replaced by incinerated municipal solid waste bottom ash. Academic Journal of Civil Engineering, 37(2), 532-538.
- Dos Santos, I. F. S., Mensah, J. H. R., Gonçalves, A. T. T., & Barros, R. M. (2020). Incineration of municipal solid waste in Brazil: An analysis of the economically viable energy potential. Renewable Energy, 149, 1386-1394.
- Elsener, B. (2001). Corrosion inhibitors for steel in concrete-State of the art report. Maney Publishing.
- Ferreira, C., Ribeiro, A., & Ottosen, L. (2003). Possible applications for municipal solid waste fly ash. Journal of hazardous materials, 96(2-3), 201-216.
- Fu, C., Jin, N., Ye, H., Jin, X., & Dai, W. (2017). Corrosion characteristics of a 4-year naturally corroded reinforced concrete beam with load-induced transverse cracks. Corrosion Science, 117, 11-23.
- Garcia-Lodeiro, I., Carcelen-Taboada, V., Fernández-Jiménez, A., & Palomo, A. (2016). Manufacture of hybrid cements with fly ash and bottom ash from a municipal solid waste incinerator. Construction and building materials, 105, 218-226.
- Ghanem, H., Machaka, M., Khatib, J., Elkordi, A., & Baalbaki, O. (2019). Effect of partial replacement of cement by MSWIBA on the properties of mortar. Academic Journal of Civil Engineering, 37(2), 82-89.
- Ghanem, H., Phelan, S., Senadheera, S., & Pruski, K. (2008). Chloride ion transport in bridge deck concrete under different curing durations. Journal of Bridge Engineering, 13(3), 218-225.
- Ghanem, H., Trad, A., Dandachy, M., & ElKordi, A. (2018, November). Effect of Wet-Mat Curing Time on Chloride Permeability of Concrete Bridge Decks. In International Congress and Exhibition on Sustainable Civil Infrastructures, (pp. 194-208). Springer, Cham.
- Hakim, A., Slika, W., El Kordi, A., & Biqai, A. (2022). A Comparative Study between the Analytical and Experimental Deflection Response of Corroded Simply Supported Reinforced Concrete Beams. In Proceedings of the 7h World Congress on Civil, Structural, and Environmental Engineering (CSEE'22).
- Harb, M. B., Abubshait, S., Etteyeb, N., Kamoun, M., & Dhouib, A. (2020). Olive leaf extract as a green corrosion inhibitor of reinforced concrete contaminated with seawater. *Arabian Journal of Chemistry*, *13*(3), 4846-4856.
- Imperatore, S., & Rinaldi, Z. (2008, September). Mechanical behaviour of corroded rebars and influence on the structural response of R/C elements. In 2nd International conference on concrete repair, rehabilitation and retrofitting (pp. 203-204). CRC PRESS-TAYLOR & FRANCIS GROUP.
- Khatib, J., Jahami, A., El Kordi, A., Sonebi, M., Malek, Z., Elchamaa, R., & Dakkour, S. (2021). Effect of municipal solid waste incineration bottom ash (MSWI-BA) on the structural performance of reinforced concrete (RC) beams. Journal of Engineering, Design and Technology.
- Lam, C. H., Ip, A. W., Barford, J. P., & McKay, G. (2010). Use of incineration MSW ash: a review. Sustainability, 2(7), 1943-1968.
- Liu J, Hu L, Tang L, Ren J (2021). Utilisation of municipal solid waste incinerator (MSWI) fly ash with metakaolin for preparation of alkali-activated cementitious material. J Hazard Mater 402:123451.
- Machaka, M., Khatib, J., Elkordi, A., Ghanem, H., & Baalbaki, O. (2019, July). Selected properties of concrete containing Municipal Solid Waste Incineration Bottom Ash (MSWI-BA). In

Proceedings of the 5th International Conference on Sustainable Construction Materials and Technologies (SCMT5), London, UK (pp. 14-17).

- Malumbela, G., Moyo, P., & Alexander, M. (2012). A step towards standardising accelerated corrosion tests on laboratory reinforced concrete specimens. Journal of the South African Institution of Civil Engineering Journal van die Suid-Afrikaanse Institute van Siviele Ingenieurswese, 54(2), 78-85.
- Nguyen, T. N., Hubbard, J. B., & MCFADDEN, G. B. (1991). A mathematical model for the cathodic blistering of organic coatings on steel immersed in electrolytes. JCT, Journal of coatings technology, 63(794), 43-52.
- Pavlík, Z., Keppert, M., Pavlíková, M., & Volfová, P. (2011). Application of MSWI bottom ash as alternative aggregate in cement mortar. WIT Transactions on Ecology and the Environment, 148, 335-342.
- Quraishi, M. A., Kumar, V., Abhilash, P. P., & Singh, B. N. (2011). Calcium stearate: A green corrosion inhibitor for steel in concrete environment. Journal of Materials and Environmental Science, 2(4), 365-372.
- Shahid, M. (2011). Corrosion protection with eco-friendly inhibitors. Advances in Natural Sciences: Nanoscience and Nanotechnology, 2(4), 043001.
- Shi, J. J., & Sun, W. (2014). Effects of phosphate on the chloride-induced corrosion behavior of reinforcing steel in mortars. Cement and Concrete Composites, 45, 166-175.
- Tang Z, Li W, Tam VWY, Xue C (2020) Advanced progress in recycling municipal and construction solid wastes for manufacturing sustainable construction materials. Resources, Conservation & Recycling X6:100036.
- Turcry, P., Oksri-Nelfia, L., Younsi, A., & Aït-Mokhtar, A. (2014). Analysis of an accelerated carbonation test with severe preconditioning. Cement and Concrete Research, 57, 70-78.
- Zhu, X., Zi, G., Cao, Z., & Cheng, X. (2016). Combined effect of carbonation and chloride ingress in concrete. Construction and Building Materials, 110, 369-380.